RESEARCH ARTICLE

J Anim Sci Technol 2021;63(5):984-997

https://doi.org/10.5187/jast.2021.e90

JAST

Journal of Animal Science and Technology

pISSN 2672-0191 eISSN 2055-0391

DNA damage repair is suppressed in porcine aged oocytes

Tao Lin[1,2], Ling Sun[1,2], Jae Eun Lee[2], So Yeon Kim[2] and Dong Il Jin[2]*

[1]*School of Life Sciences and Food Engineering, Hebei University of Engineering, Handan 056038, China*

[2]*Division of Animal & Dairy Science, Chungnam National University, Daejeon 34134, Korea*

Received: Jun 4, 2021
Revised: Jul 1, 2021
Accepted: Jul 9, 2021

***Corresponding author**
Dong Il Jin
Division of Animal & Dairy Science, Chungnam National University, Daejeon 34134, Korea.
Tel: +82-42-821-5876
E-mail: dijin@cnu.ac.kr

ORCID
Tao Lin
https://orcid.org/0000-0001-9100-6042
Ling Sun
https://orcid.org/0000-0001-5160-2122
Jae Eun Lee
https://orcid.org/0000-0003-1435-5980
So Yeon Kim
https://orcid.org/0000-0001-8080-3126
Dong Il Jin
https://orcid.org/0000-0001-6586-4393

Competing interests
No potential conflict of interest relevant to this article was reported.

Funding sources
This work was supported by a National Research Foundation of Korea (NRF) grant funded by the Ministry of Education, Science and Technology (MEST) of the Korean government (NRF-2019R1I1A3A01061877).

Acknowledgements
Not applicable.

Abstract

This study sought to evaluate DNA damage and repair in porcine postovulatory aged oocytes. The DNA damage response, which was assessed by H2A.X expression, increased in porcine aged oocytes over time. However, the aged oocytes exhibited a significant decrease in the expression of RAD51, which reflects the DNA damage repair capacity. Further experiments suggested that the DNA repair ability was suppressed by the downregulation of genes involved in the homologous recombination (HR) and nonhomologous end-joining (NHEJ) pathways. The expression levels of the cell cycle checkpoint genes, *CHEK1* and *CHEK2*, were upregulated in porcine aged oocytes in response to induced DNA damage. Immunofluorescence results revealed that the expression level of H3K79me2 was significantly lower in porcine aged oocytes than in control oocytes. In addition, embryo quality was significantly reduced in aged oocytes, as assessed by measuring the cell proliferation capacity. Our results provide evidence that DNA damage is increased and the DNA repair ability is suppressed in porcine aged oocytes. These findings increase our understanding of the events that occur during postovulatory oocyte aging.

Keywords: Oocyte aging, DNA damage, DNA repair, H3K79me2, Pig

INTRODUCTION

Oocyte aging is associated with a range of morphological, cellular and molecular changes that lead to deterioration during the aging period and negatively influence oocyte quality and subsequent embryo development in mouse [1–5], human [6,7], pig [8] and bovine [9]. Extensive studies have shown the following: The morphological changes in aged oocytes include zona pellucida hardening [10], perivitelline space enlargement [11], polar body degeneration or drifting [11] and spontaneous oocyte activation [12]. The cellular changes in aged oocytes include partial cortical granule exocytosis [13], microfilament loss [14], spindle mispairing [15] and chromosomal aneuploidy [16]. The molecular changes in aged oocytes include mitochondrial dysfunction [17,18], activity decreases of mitogen-activated protein kinase and maturation promoting factor [19], increases in reactive oxygen species [20], enhancement of apoptosis [21], alteration of DNA methylation [22] and histone modifications [23]. Together, these studies provide very important references for understanding the events that occur during oocyte aging in many species.

DNA damage includes DNA single-strand breaks (SSBs) and double-strand breaks (DSBs). The

Availability of data and material
Upon reasonable request, the datasets of this study can be available from the corresponding author.

Authors' contributions
Conceptualization: Lin T, Sun L, Jin DI.
Data curation: Lin T, Lee JE, Jin DI.
Formal analysis: Lin T, Sun L.
Methodology: Lin T, Lee JE, Kim SY.
Validation: Lee JE, Kim SY.
Writing - original draft: Lin T, Jin DI.
Writing - review & editing: Lin T, Jin DI.

Ethics approval and consent to participate
Animal experiments were approved by the Institutional Animal Care and Use Committee of Chungnam National University, Korea (202003A-CNU-002).

latter are generally recognized as the most important form of DNA damage [24], and should activate DNA repair and DNA damage checkpoint mechanisms [25]. DNA damage checkpoint mechanisms arrest cell division until all DNA damage is repaired [26]. However, if the damage cannot be repaired by the DNA repair mechanisms, the cell can proceed to various outcomes, including mutagenesis, cell senescence and apoptosis [27]. There are two main pathways responsible for DSB repair: homologous recombination (HR) and nonhomologous end-joining (NHEJ). In response to DNA damage, the ATM (ataxia telangiectasia mutated) and ATR (ataxia telangiectasia and rad3 related) proteins are responsible for phosphorylating histone H2A.X (H2A.X139ph) at the sites of the DNA DSBs [28,29]. The phosphorylation of histone H2A.X is closely linked to DNA DSBs repair, because the phosphorylated histone serves as a platform for the accumulation of DNA repair proteins involved in the HR (RAD51, MRE11A, BRCA1) or NHEJ (PRKDC, XRCC4, DNA ligase IV, 53BP1) pathways, which can colocalize with H2A.X at the sites of DNA DSBs [30,31].

Recently, a growing body of scientific evidence has suggested that aging is linked to the DNA damage response and DNA damage repair ability. For instance, increased DNA damage and reduced DNA damage repair in rhesus monkey granulosa cells [32] and human oocytes [33] has been associated with ovarian aging. Compared with the existing knowledge regarding somatic cells or oocytes derived from aged ovaries (reproductive or maternal aging), however, relatively little is known about the DNA damage and repair responses in postovulatory aged oocytes (postovulatory aging). A recent study that used H2A.X staining to investigate DNA damage in mice postovulatory aged oocytes found that the DNA damage level was significantly increased in mice aged oocytes [34]. However, the underlying molecular mechanisms have not been fully elucidated.

Here, we used the porcine oocyte as a model to investigate the involvement of DNA damage and repair in the function of postovulatory aging oocytes. To this end, we evaluated: 1) the levels of H2A.X and RAD51 proteins, which reflect the damage response and repair capacity, respectively; 2) the mRNA expression levels of genes involved in the HR (*ATR*, *ATM*, *MRE11A*, *RAD51* and *RAD52*) and NHEJ (*XRCC4*, *XRCC5*, *XRCC6*, *PRKDC* and *LIG4*) pathways of DNA repair; 3) the mRNA abundance of genes involved in cell cycle control (*CHK1* and *CHK2*); 4) the level of H3K79me2 in aged oocytes; and 5) the embryonic developmental capacity of porcine aged oocytes.

MATERIALS AND METHODS

Chemicals/reagents and animal ethics statement

All utilized chemicals and reagents were obtained from Sigma (St. Louis, MO, USA) unless otherwise stated. All animal experiments were approved by the Institutional Animal Care and Use Committee (IACUC) of Chung Nam National University, Korea (202003A-CNU-002).

Oocyte collection

Porcine ovaries were obtained from a local abattoir and transported to the laboratory in physiological saline at 35℃ within 2 h of collection. Follicular contents were aspirated from antral follicles (3 to 6 mm in diameter) visible on the ovarian surface using an 18-gauge needle attached to a 10-ml disposable syringe. Cumulus oocyte complexes (COCs) were collected and washed two or three times in phosphate-buffered saline (PBS) (Gibco, USA) containing 0.1% polyvinyl alcohol (PVA). Only oocytes with a uniform ooplasm and compact cumulus cell mass were used for *in vitro* maturation.

In vitro maturation (IVM) and *in vitro* aging (IVA) of porcine oocytes

For IVM, the COCs were washed three times and groups of about 50~60 COCs were matured in 500 μL maturation medium (tissue culture medium [TCM] 199 containing 10% porcine follicular fluid, 3.5 mM D-glucose, 0.57 mM L-cysteine, 0.91 mM sodium pyruvate, 75 μg/mL penicillin, 50 μg/mL streptomycin, 10 ng/mL epidermal growth factor, 10 IU/mL pregnant mare serum gonadotropin, 10 IU/mL human chorionic gonadotropin) in each well of a four-well multi dish in saturated-humidity air containing 5% CO_2 at 38.5℃ for 44 h. For IVA, oocyte aging was performed as described previously [35]. In brief, the matured porcine oocytes were cultured in the same medium and condition for an extended period of 24 h (IVA 24 h) or 48 h (IVA 48 h) to mimic postovulatory oocyte aging. After oocyte IVM or IVA, we removed cumulus cells from COCs by pipetting or vortexing them in 0.1% hyaluronidase solution. Survival of oocytes was investigated under a stereomicroscope based on oocyte morphology. Only oocytes with integrated oolemma and zona pellucida and a polar body were used for experiments, whereas those with lysis of the oolemma or damage to the zona pellucida or cytoplasmic fragmentation were considered to discard.

Embryo production by parthenogenetic activation (PA)

For PA, the oocytes were subjected to electrical activation. Cumulus cell-free oocytes were washed three times and then equilibrated in an activation solution containing 0.3 M D-mannitol, 0.1 mM $MgSO_4$, 0.05 mM $CaCl_2$ and 0.01% PVA. The oocytes were placed between the platinum electrodes in activation solution, and activation was induced with two direct current pulses of 1.1 kV/cm for 30 μs, using an Electro Cell Manipulator 2001 (BTX, San Diego, CA, USA). After electric stimulation, the oocytes were cultured in porcine zygote medium-3 containing 3 mg/mL bovine serum albumin (BSA) and 7.5 μg/mL cytochalasin B (CB) for 5 h (to inhibit extrusion of the second polar body) at 38.5℃ in a humid 5% CO_2 atmosphere. After 5 h incubation with CB, the embryos were transferred to CB-free culture medium for further culture.

General immunofluorescence staining

Immunofluorescence staining was performed as described previously [36]. Briefly, oocytes were washed in PBS-PVA and then fixed in 4% paraformaldehyde for 30 min. After being permeabilized with 0.5% (v/v) Triton X 100 in PBS-PVA for 30 min, they were blocked with 3% BSA for 1 h. Samples were washed in PBS containing 0.5% BSA and 0.1% gelatin (PBG), and incubated overnight at 4℃ with primary antibodies. The samples were washed in PBG and then reacted with secondary antibodies in the dark for 1 h. After being washed with PBG, the samples were mounted on glass slides using VECTASHIELD mounting medium with 4',6-diamidino-2-phenylindole (DAPI) (Vector Laboratories, Burlingame, CA, USA) and viewed under a Zeiss laser-scanning confocal microscope (LSM5 Live, Carl Zeiss, Oberkochen, Baden-Württemberg, Germany). Negative control embryos were processed as described above, except that no primary antibody was added. The utilized primary antibodies recognized H2A.X (Merck KGaA, Darmstadt, Germany), RAD51 (Santa Cruz Biotechnology, Dallas, TX, USA), H3K79me2 (Abcam, Cambridge, UK), and H3 (Active Motif, Carlsbad, CA, USA). The utilized secondary antibodies were goat anti-mouse IgG-R (Santa Cruz Biotechnology), goat anti-mouse IgG-FITC (Santa Cruz Biotechnology), or donkey anti-rabbit FITC (Abcam).

5-ethynyl-2'-deoxyuridine (EdU) labeling

EdU staining was performed using a Click-iT EdU Imaging kit (Invitrogen, Eugene, OR, USA). The provided manufacturer's instructions are normally intended for use in cell culture, but the

https://doi.org/10.5187/jast.2021.e90

protocol was adapted for porcine embryos as follows. Briefly, porcine blastocysts were collected and incubated in EdU (10 μM) solution for 3 h, and then fixed in 4% paraformaldehyde for 15 min. After being washed with 3% BSA, samples were permeabilized with 0.5% Triton X-100 for 20 min. The samples were again washed with 3% BSA and then reacted with a Click-iT reaction cocktail containing Click-iT reaction buffer, $CuSO_4$, reaction buffer additive and Alexa Fluor 488 azide for 30 min in the dark. After EdU detection, the samples were washed and mounted on glass slides using VECTASHIELD mounting medium containing DAPI. Images were captured using a Zeiss laser-scanning confocal microscope.

RNA isolation and real-time quantitative polymerase chain reaction (PCR)

Total RNA was extracted from each sample (200 oocytes) using an RNeasy Mini Kit (Qiagen, Valencia, CA, USA) and an RNase-Free DNase Set (Qiagen) in accordance with the manufacturer's instructions. cDNA was synthesized from the isolated total RNA using a TOPscript™ RT DryMIX kit (Enzynomics, Daejeon, Korea). Quantitative real-time PCR was performed using a TOPreal™ qPCR 2X PreMIX (SYBR Green with low ROX) kit (Enzynomics) on a CFX96 Touch Real-Time PCR Detection System (Bio-Rad, St. Ingbert, Germany). PCR controls run with no template were performed for each primer pair. Finally, the relative mRNA expression levels of each gene were analyzed using the $2^{-\Delta\Delta Ct}$ method [37]. The primer sequences used for real-time PCR are presented in Table 1.

Table 1. The information and primer sequence of genes used in this study

Gene	Primer sequence (5'→3')	Annealing temp (℃)	Accession number
MRE11A	F: GGAGGATGTTGTCCTGGCTG R: AGACGTTCCCGTTCTGCATT	55	XM_003129789.2
PRKDC	F: ATTCTTTGTCGGGAGCAGCA R: CCTAGCTGTGTGGCACATGA	55	XM_001925309.4
RAD51	F: CTTCGGTGGAAGAGGAGAGC R: CGGTGTGGAATCCAGCTTCT	55	NM_001123181.1
RAD52	F: ATTCAGCAAGGGATGCCCAC R: TAGGGCAAGGGCGTTTTCTT	55	XM_003358103.2
ATM	F: CCGGTGTTTTGGGAGAGTGT R: CTTCCGACCAAACTCAGCGT	55	NM_001123080.1
ATR	F: TGAGCTCCAGTGTTGGCATC R: GCCAGTTCTCAGTGTGGTCA	55	XM_003132459.3
XRCC4	F: ATGGCTTCACAGGAGCTTCA R: ATGTTTTCAGCTGGGCTGTG	55	XM_003123760.2
XRCC5	F: CTGGCATCTCGCTGCAATTC R: GAAAGGAGGGTCCATGGTGG	55	XM_003133649.2
XRCC6	F: ACGGAAGGTGCCCTTTACTG R: TGCAGCACTGGGTTCTCAAA	55	NM_001190185.1
LIG4	F: AGCTAGACGGCGAACGTATG R: CCTTCCTGTGGGGAAACTCC	55	XM_003131089.2
CHEK1	F: TGCCCTTTGTGGAAGACTGG R: ACTGCAACTGCTTCCTCAGT	55	XM_003130047.2
CHEK2	F: GCCTGTGGTGAGGTGAAACT R: TGCTGGATCTGCCTCTCTCT	55	NM_001137638.1
ACTB	F: GTGGACATCAGGAAGGACCTCTA R: ATGATCTTGATCTTCATGGTGCT	55	U_07786
GAPDH	F: GCCATCACCATCTTCCAGG R: TCACGCCCATCACAAACAT	55	NM_001206359.1

F, forward; R, reverse.

Experimental design

Experiment 1. Examining DNA damage and repair in porcine aged oocytes

DNA damage was detected by detecting DNA double strands breaks using an antibody against H2A.X. Four independent experiments were performed, and total 40 (Control), 42 (IVA 24 h), 46 (IVA 48 h) oocytes were analyzed. DNA repair was evaluated using an antibody against RAD51. Three independent experiments were performed, and total 30 (Control), 30 (IVA 24 h), 30 (IVA 48 h) oocytes were analyzed in this set of experiment. Fluorescence intensities were analyzed, and the background value was subtracted using the ImageJ software.

Experiment 2. Examining transcript levels for DNA repair and cell cycle checkpoint-related genes in porcine aged oocytes

Expression levels of genes involved in the HR (*ATR*, *ATM*, *MRE11A*, *RAD51* and *RAD52*) and NHEJ (*XRCC4*, *XRCC5*, *XRCC6*, *PRKDC* and *LIG4*) pathways for DNA damage repair and cell cycle checkpoint (*CHEK1* and *CHEK2*) in porcine aged oocytes were investigated using real-time quantitative PCR. Three independent experiments were performed in this set of experiment. Each experimental group contains about 200 oocytes were used for total RNA extraction.

Experiment 3. Examining expression levels of H3K79me2 and H3 in porcine aged oocytes

The expression of H3K79me2 was detected using antibody against H3K79me2. Four independent experiments were performed, and total 48 (Control), 52 (IVA 24 h), 52 (IVA 48 h) oocytes were analyzed. The expression of H3 was detected using antibody against H3. Three independent experiments and total 30 (Control), 30 (IVA 24 h), 30 (IVA 48 h) oocytes were analyzed. Immunofluorescence intensities were analyzed, and the background value was subtracted using the ImageJ software.

Experiment 4. Examining development of porcine aged oocytes after PA

Developmental capacity and cell proliferation potential were investigated using morphology and EdU staining. Blastocyst morphology pictures were captured under a stereomicroscope with an ocular scale at day 7 of culture, and diameter of blastocyst was measured using the ImageJ software. At least three independent experiments were performed for each study. Total 189 (Control), 180 (IVA 24 h), 193 (IVA 48 h) oocytes were analyzed for embryo development. Total 64 (Control), 45 (IVA 24 h) blastocysts were analyzed for blastocyst diameter. Total 20 (Control), 15 (IVA 24 h) blastocysts were analyzed for cell proliferation potential in blastocyst. Because IVA 48 h group failed to develop to blastocyst stage, the analyses presented in both diameter and cell proliferation potential of blastocyst were not performed for the IVA 48 h group.

Statistical analysis

Statistical analyses were conducted using SPSS 17.0 (SPSS, Chicago, IL, USA). At least three replicates were performed for each experiment. Percentage data were subjected to arcsine transformation prior to analysis. All experimental data were compared by one-way ANOVA followed by Fisher's protected least significant difference test or Student's *t*-test. The data are expressed as the mean ± sem. $p < 0.05$ was considered significantly different.

RESULTS

Increased DNA damage and decreased DNA repair in porcine aged oocytes

We first assessed the DNA damage response protein, H2A.X139ph, to evaluate the DNA DSB

https://doi.org/10.5187/jast.2021.e90

response in porcine aged oocytes. The fluorescence signals of H2A.X139ph (green) could be detected in all porcine oocytes (Fig. 1A); however, a higher level of DNA damage response was observed in porcine aged oocytes (IVA 24 h and IVA 48 h) than in control oocytes (Fig. 1B). To examine the activity of the DNA damage repair response during the oocyte aging period, we immunostained for RAD51 in porcine aged oocytes. The fluorescence signals of RAD51 (red) could be detected in porcine oocytes (Fig. 1C), and the relative intensities of fluorescence signals were significantly lower in aged oocytes than in controls (Fig. 1D).

Transcript levels for DNA repair-related genes in porcine aged oocytes

To test whether the increased DNA damage in aged oocytes could be related to a deficiency of DNA damage repair, we measured the mRNA abundances of genes involved in the HR (*ATR*, *ATM*, *MRE11A*, *RAD51* and *RAD52*) and NHEJ (*XRCC4*, *XRCC5*, *PRKDC*, *LIG4 and XRCC6*) pathways of DNA damage repair in porcine aged oocytes. The levels of various genes involved in the HR repair pathway were found to be significantly decreased in the IVA 24 h group (*ATR*,

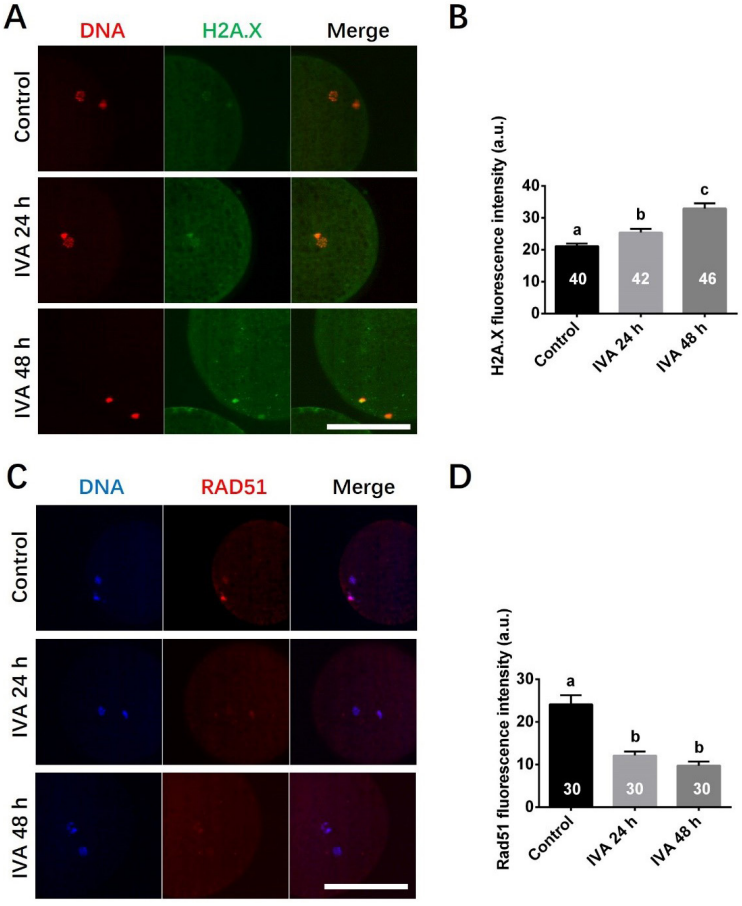

Fig. 1. DNA damage and repair in porcine aged oocytes. (A) DNA damage was evaluated by detecting DNA double strands breaks using an antibody against H2A.X (green), and DNA was stained with DAPI (red). (B) Quantitative analysis of levels of DNA damage (H2A.X fluorescence intensity) in the nuclei of oocytes (including polar bodies). (C) DNA damage repair was detected using an antibody against RAD51 (red) and DNA was stained with DAPI (blue). (D) Quantitative analysis of DNA damage repair (RAD51 fluorescence intensity) in the nuclei of oocytes (including polar bodies). The numbers of embryos tested in each group are shown as bars. $^{a-c}$Different letters above the bars indicate statistically significant differences ($p < 0.05$). Scale bars represent 50 μm in A and C. IVA, in vitro aging; DAPI, 4',6-diamidino-2-phenylindole.

MRE11A and *RAD52*) and/or IVA 48 h group (*ATR*, *ATM*, *MRE11A*, *RAD51* and *RAD52*) when compared to controls (Fig. 2A). The expression levels of various genes involved in the NHEJ pathway were also significant lower in the IVA 24 h group (*XRCC4*, *PRKDC* and *LIG4*) or IVA 48 h group (*XRCC4*, *XRCC5*, *PRKDC* and *LIG4*) than in controls (Fig. 2B). However, there was no difference in the level of the *XRCC6* gene between the control and aged oocyte groups (Fig. 2B).

Transcript levels of cell cycle checkpoint-related genes in porcine aged oocytes

The transcript levels of the cell cycle checkpoint genes *CHEK1* and *CHEK2* were also estimated in porcine aged oocytes (Fig. 3). The mRNA level of *CHEK1* was significantly higher in aged oocytes (both IVA 24 and 48 h) than in controls (Fig. 3A). The expression level of *CHEK2* did not significantly differ between the IVA 24 h group and the control group, but it was significantly increased in the IVA 48 h group compared to the control group (Fig. 3B).

The expression levels of H3K79me2 and H3 in porcine aged oocytes

The expression levels of H3K79me2 and H3 were examined in porcine aged oocytes, as shown in Fig. 4. Immunofluorescence revealed that the expression level of H3K79me2 was significantly decreased in porcine aged oocytes (IVA 24 h and IVA 48 h) when compared to controls (Figs. 4A and B). In contrast, H3 exhibited similar expression levels in the control, IVA 24 h and IVA 48 h groups (Figs. 4C and D).

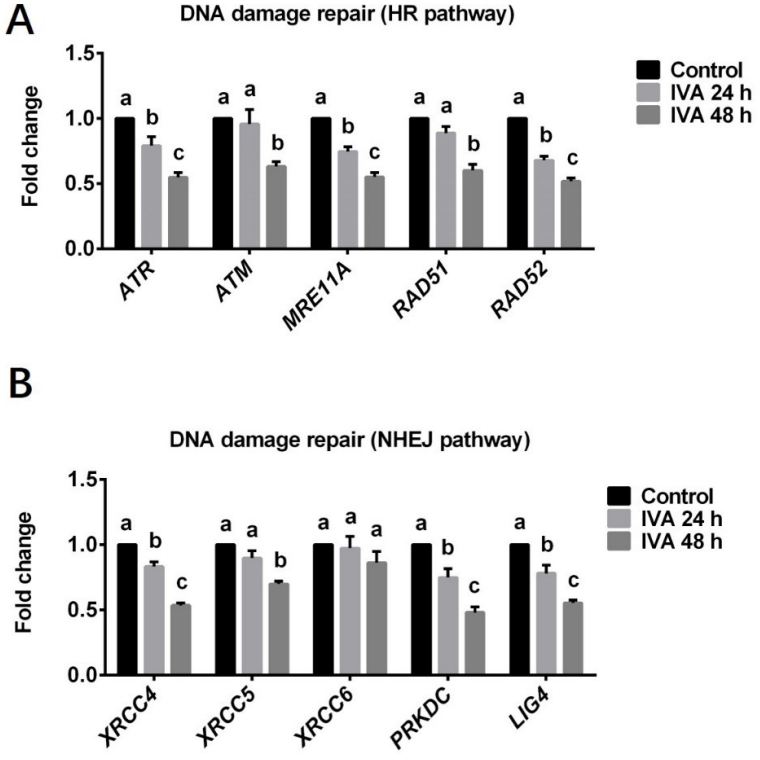

Fig. 2. Transcript levels for DNA repair-related genes in porcine aged oocytes. (A) Expression levels of genes involved in the HR pathway for DNA damage repair in porcine aged oocytes. (B) Expression levels of genes involved in the NHEJ pathway for DNA damage repair in porcine aged oocytes. [a–c]Different letters above the bars indicate statistically significant differences ($p < 0.05$). HR, homologous recombination; ATR, ataxia telangiectasia and rad3 related; ATM, ataxia telangiectasia mutated; IVA, *in vitro* aging; NHEJ, nonhomologous end-joining.

https://doi.org/10.5187/jast.2021.e90

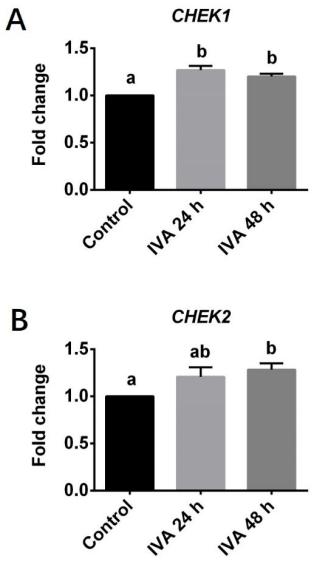

Fig. 3. Transcript levels of cell cycle checkpoint-related genes in porcine aged oocytes. (A) Expression level of *CHEK1* in porcine aged oocytes. (B) Expression level of *CHEK2* in porcine aged oocytes. [a,b]Different letters above the bars indicate statistically significant differences ($p < 0.05$). IVA, *in vitro* aging.

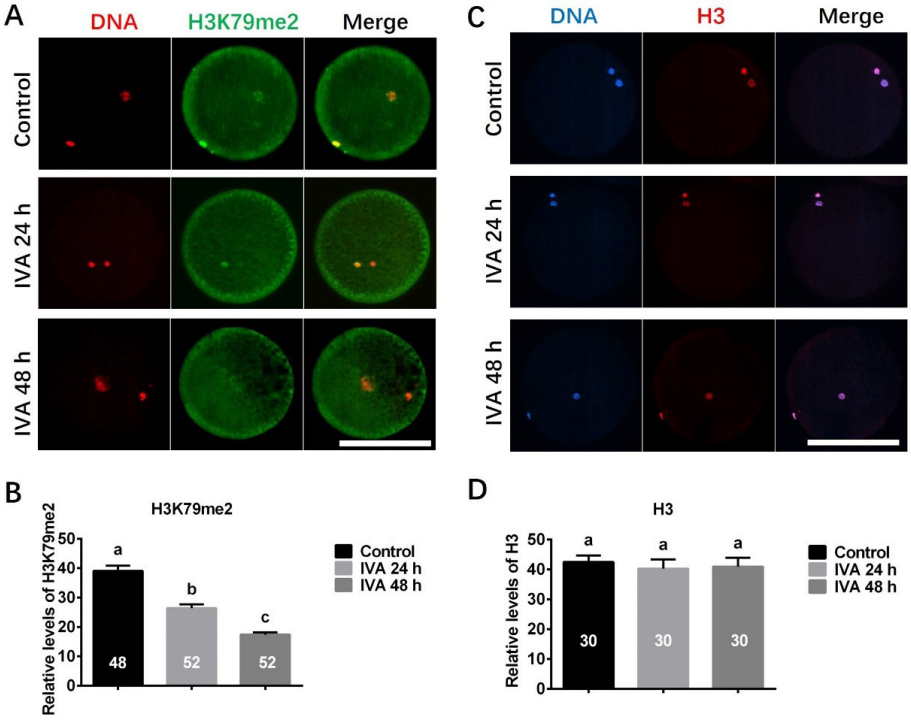

Fig. 4. The expression levels of H3K79me2 and H3 in porcine aged oocytes. (A) Images of oocytes immunostained for H3K79me2 (green). DNA was stained with DAPI (red). (B) Quantitative analysis of H3K79me2 in the nuclei of oocytes (including polar bodies). (C) Images of oocytes immunostained for H3 (red). DNA was stained with DAPI (blue). (D) Quantitative analysis of H3 in the nuclei of oocytes (including polar bodies). The numbers of samples tested in each group are shown as bars. [a–c]Different letters above the bars indicate statistically significant differences ($p < 0.05$). Scale bars represent 100 μm in A and C. IVA, *in vitro* aging; DAPI, 4',6-diamidino-2-phenylindole.

Poor development of porcine aged oocytes

The embryo development capacity was significantly reduced in the aged oocyte groups compared to controls (Fig. 5). Embryos derived from the IVA 24 h group could develop to the blastocyst stage, but the rate of blastocyst formation was significantly lower than in the control group (Figs. 5A and B). Blastocysts derived from the IVA 24 h group also had smaller diameters than those derived from control oocytes (Fig. 5C). In contrast, no blastocyst formation was observed among the IVA 48 h group, and more than half of the derived embryos arrested at the 2-cell stage by day 7 of culture (Figs. 5A and B). EdU staining showed that the total cell number (TC), the EdU-positive (S-phase) cell number and the ratio of EdU-positive cells to TC were significantly lower in blastocysts derived from the IVA 24 h group compared to the control values (Figs. 5D and E).

DISCUSSION

Oocyte aging is known to negatively influence oocyte quality, embryonic development and reproductive outcomes. However, the underlying molecular mechanisms have not been fully elucidated. In the present study, we investigated whether the DNA damage response and DNA damage repair ability are closely linked to oocyte aging. Our results showed that postovulatory oocyte aging increased the DNA damage response and suppressed the DNA damage repair

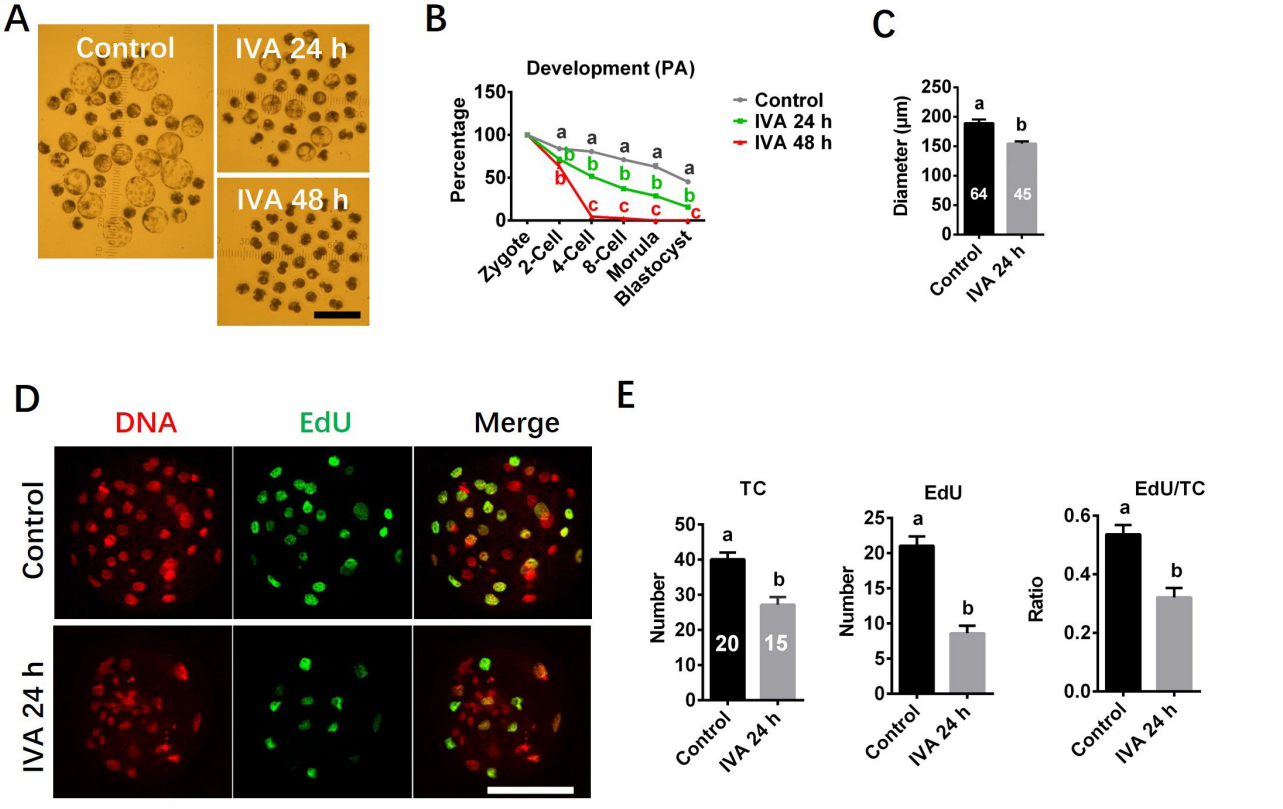

Fig. 5. Developmental capacity of porcine aged oocytes. (A) Images of embryos derived from the control, IVA 24 h and IVA 48 h groups. (B) Developmental potential of porcine embryos. Because IVA 48 h group failed to develop to blastocyst stage, the analyses presented in panel C, D and E were not performed for the IVA 48 h group. (C) Diameter of blastocysts. (D) EdU staining of porcine blastocysts. The green fluorescence shows EdU-positive cells and red fluorescence shows all nuclei of blastocysts. (E) TC, EdU-positive cell number and the ratio of the EdU-positive cell number to the TC. The numbers of embryos tested in each group are shown as bars. $^{a-d}$Different letters above the bars indicate statistically significant differences ($p < 0.05$). Scale bars represent 500 μm in A and 100 μm in D. IVA, *in vitro* aging; PA, parthenogenetic activation; TC, total cell number; EdU, 5-ethynyl-2'-deoxyuridine.

https://doi.org/10.5187/jast.2021.e90

capacity in porcine oocytes. The development of therapies that target these signaling pathways might help prevent or delay oocyte aging.

Previous reports suggested that an increased DNA damage response and reduced DNA repair capacity in rhesus monkey granulosa cells [32] or mouse and human oocytes [33] may contribute to ovarian aging. In mouse aged oocytes derived from an *in vitro* aging model, researchers observed a considerable increase in the level of DNA damage in comparison with control oocytes [34]. However, the previous studies had notable limitations, such as the use of oocytes or cells from aged ovaries or the use of H2A.X staining alone to evaluate the DNA damage response. Here, in a pig *in vitro* oocyte aging model, we first assessed the DNA damage response marker, H2A.X, and the repair protein, RAD51, in porcine aged oocytes. The presence of phosphorylated histone H2A.X (H2A.X 139ph) foci has been widely used to estimate the occurrence of DNA damage in somatic cells [38,39], oocytes [40] and embryos [25,31]. RAD51, a recA homolog that binds the single-strand DNA generated by the Mre11-Rad50-NBS1 complex, is a key factor for DNA damage repair [41]. In the present study, porcine oocytes showed an appreciable H2A.X signal (consistent with an active DNA damage response) that increased in intensity as the oocytes aged, indicating that the incidence of DNA damage in porcine oocytes increased with the aging time. Conversely, the protein expression of RAD51, which reflects the damage repair ability, decreased in aged oocytes over time. Our results suggest that oocyte aging increases DNA damage and suppresses the DNA damage repair ability in pig.

To further evaluate the influence of oocyte aging on the DNA damage repair ability, we investigated the mRNA expression levels of genes involved in the NHEJ (*XRCC4*, *XRCC5*, *XRCC6*, *PRKDC* and *LIG4*) and HR (*ATR*, *ATM*, *MRE11A*, *RAD51* and *RAD52*) pathways in porcine aged oocytes. Our results showed that the relative mRNAs abundance of the genes (except *XRCC6*) involved in the two repair pathways decreased over time in porcine aged oocytes, suggesting that these two DNA damage repair pathways are suppressed in this model. However, there was no difference in the level of the *XRCC6* gene between control and aged oocytes, and it is speculated that porcine oocyte aging *in vitro* suppresses DNA damage repair ability probably not by *XRCC6* gene product. Consistent with our results, previous studies that examined the relationship between DNA damage repair and ovarian aging in human oocytes [24] and rat primordial follicles [42] found that the expression levels of some important DNA repair genes (e.g., *BRCA1*, *RAD51* and *MRE11*) declined with age. Together, the previous and present results suggest that it may be difficult for the DNA damage repair mechanisms to repair aging-induced DNA damage. Supplementation of antiaging chemicals Coenzyme Q10 and melatonin could reduce DNA damage in mice [34] and bovine [9] aged oocytes by detecting DNA double strands breaks using an antibody against H2A.X had been already reported. However, there is little evidence that adding antiaging chemicals improves DNA damage repair ability. Future work is needed to examine whether the DNA repair ability could be improved by using antiaging treatment in oocytes.

Cell cycle checkpoint kinase 1 (Chk1) and 2 (Chk2) are well known to be activated by the ATM and ATR kinases in response to DNA damage; this leads to cell cycle arrest, which allows the cell sufficient time to repair the damaged DNA before it undergoes replication and segregation in cleaving cells [25,43,44]. Once the DNA damage repair is complete, the cell cycle checkpoint proteins are inactivated and the cell cycle resumes. In the current study, we found that the mRNA expression levels of *CHEK1* and *CHEK2*, which encode Chk1 and Chk2, respectively, were increased along with the DNA damage response in porcine aged oocytes compared to controls. This is in line with previous observations that *CHEK1* and *CHEK2* are activated in mouse [45] and pig [25] embryos that have increased levels of DNA damage. The *CHEK1* and *CHEK2* genes are usually activated to enable the damaged DNA to be repaired. However, we found that the

expression levels of DNA damage repair-related proteins and genes were decreased in aged oocytes. We speculate that the long-term arrest of aged oocytes at metaphase II stage may allow DNA damage accumulate to a level at which the DNA damage repair ability becomes suppressed.

Epigenetics has recently emerged as another possible determinant of (and potentially a major contributor to) the aging phenotype [46]. Generally, changes in histone methylation are related to the activation/repression of gene transcription [47]. H3K79me2, which has been suggested as a marker of active genes in mammalian cells [48], and is also thought to be associated with the DNA damage repair mechanism [49]. Here, we found that the expression level of H3K79me2 in porcine oocytes was obviously decreased during *in vitro* postovulatory aging. We speculate that this may be associated with the observed deficiency in the DNA damage repair mechanism of porcine aged oocytes.

Previous studies found that laser microbeam-induced DNA damage in mouse embryos reduced the rates of cleavage and blastocyst formation [45], and the incidence of the DNA damage response is higher and developmental capacity is lower in late-cleaving porcine embryos than in their early-cleaving counterparts [25]. The above studies imply that there is a negative relationship between DNA damage and embryo development. In the present study, we found that embryos derived from aged oocytes have decreased developmental abilities: the IVA 24 h group showed a decreased ability to develop to the blastocyst stage, while the IVA 48 h group failed to develop to the blastocyst stage, with more than half of the embryos arresting at the 2 cell stage. Thus, we speculated that the presence of DNA damage induced by oocyte aging could be one of the reasons causing embryo development impaired. Moreover, consistent with previous reports that the kinetics of cleaving [25] and blastocyst formation [50] can influence the total cell number in blastocysts, we found that blastocysts derived from aged oocytes possess lower total cell and EdU-positive cell numbers than controls. Thus, we suggest that oocyte aging suppresses the cell proliferation capacity in porcine blastocysts.

In conclusion, we herein demonstrate that oocyte aging increased the DNA damage response in porcine aged oocytes as indicated by upregulation of H2A.X expression. However, the DNA damage repair ability was suppressed in porcine aged oocytes matured *in vitro*, downregulation of the RAD51 protein level and the mRNA expression levels of genes involved in both HR and NHEJ pathways. The expression levels of the cell cycle checkpoint genes, *CHKE1* and *CHKE2*, were upregulated in porcine aged oocytes in response to induced DNA damage. The H3K79me2 level decreased in porcine oocytes during *in vitro* postovulatory aging. In addition, postovulatory oocyte aging altered the kinetics of both cleavage and blastocyst formation and suppressed the cell proliferation capacity in blastocysts. These results provide useful information to help us understand the internal events that govern oocyte aging and thus may be targeted to delay oocyte aging.

REFERENCES

1. Sun SC, Gao WW, Xu YN, Jin YX, Wang QL, Yin XJ, et al. Degradation of actin nucleators affects cortical polarity of aged mouse oocytes. Fertil Steril. 2012;97:984-90. https://doi.org/10.1016/j.fertnstert.2012.01.101
2. Liang QX, Lin YH, Zhang CH, Sun HM, Zhou L, Schatten H, et al. Resveratrol increases resistance of mouse oocytes to postovulatory aging in vivo. Aging (Albany NY). 2018;10:1586-96. https://doi.org/10.18632/aging.101494
3. Wang Y, Li L, Fan LH, Jing Y, Li J, Ouyang YC, et al. N-acetyl-L-cysteine (NAC) delays post-ovulatory oocyte aging in mouse. Aging (Albany NY). 2019;11:2020-30. https://doi.org/10.18632/aging.101898

https://doi.org/10.5187/jast.2021.e90

4. Miao YL, Kikuchi K, Sun QY, Schatten H. Oocyte aging: cellular and molecular changes, developmental potential and reversal possibility. Hum Reprod Update. 2009;15:573-85. https://doi.org/10.1093/humupd/dmp014
5. Bertoldo MJ, Listijono DR, Ho WHJ, Riepsamen AH, Goss DM, Richani D, et al. NAD+ repletion rescues female fertility during reproductive aging. Cell Rep. 2020;30:1670-81. https://doi.org/10.1016/j.celrep.2020.01.058
6. Wilcox AJ, Weinberg CR, Baird DD. Post-ovulatory ageing of the human oocyte and embryo failure. Hum Reprod. 1998;13:394-7. https://doi.org/10.1093/humrep/13.2.394
7. Liu MJ, Sun AG, Zhao SG, Liu H, Ma SY, Li M, et al. Resveratrol improves in vitro maturation of oocytes in aged mice and humans. Fertil Steril. 2018;109:900-7. https://doi.org/10.1016/j.fertnstert.2018.01.020
8. Wang T, Gao YY, Chen L, Nie ZW, Cheng W, Liu X, et al. Melatonin prevents postovulatory oocyte aging and promotes subsequent embryonic development in the pig. Aging (Albany NY). 2017;9:1552-64. https://doi.org/10.18632/aging.101252
9. Liang S, Guo J, Choi JW, Kim NH, Cui XS. Effect and possible mechanisms of melatonin treatment on the quality and developmental potential of aged bovine oocytes. Reprod Fertil Dev. 2017;29:1821-31. https://doi.org/10.1071/RD16223
10. Xu Z, Abbott A, Kopf GS, Schultz RM, Ducibella T. Spontaneous activation of ovulated mouse eggs: time-dependent effects on M-phase exit, cortical granule exocytosis, maternal messenger ribonucleic acid recruitment, and inositol 1,4,5-trisphosphate sensitivity. Biol Reprod. 1997;57:743-50. https://doi.org/10.1095/biolreprod57.4.743
11. Miao Y, Ma S, Liu X, Miao D, Chang Z, Luo M, et al. Fate of the first polar bodies in mouse oocytes. Mol Reprod Dev. 2004;69:66-76. https://doi.org/10.1002/mrd.20148
12. Lord T, Nixon B, Jones KT, Aitken RJ. Melatonin prevents postovulatory oocyte aging in the mouse and extends the window for optimal fertilization in vitro. Biol Reprod. 2013;88:67. https://doi.org/10.1095/biolreprod.112.106450
13. Ducibella T, Duffy P, Reindollar R, Su B. Changes in the distribution of mouse oocyte cortical granules and ability to undergo the cortical reaction during gonadotropin-stimulated meiotic maturation and aging in vivo. Biol Reprod. 1990;43:870-6. https://doi.org/10.1095/biolreprod43.5.870
14. Kim NH, Moon SJ, Prather RS, Day BN. Cytoskeletal alteration in aged porcine oocytes and parthenogenesis. Mol Reprod Dev. 1996;43:513-8. https://doi.org/10.1002/(SICI)1098-2795(199604)43:4<513::AID-MRD14>3.0.CO;2-%23
15. Goud AP, Goud PT, Van Oostveldt P, Diamond MP, Dhont M. Dynamic changes in microtubular cytoskeleton of human postmature oocytes revert after ooplasm transfer. Fertil Steril. 2004;81:323-31. https://doi.org/10.1016/j.fertnstert.2003.06.033
16. Hornak M, Jeseta M, Musilova P, Pavlok A, Kubelka M, Motlik J, et al. Frequency of aneuploidy related to age in porcine oocytes. PLOS ONE. 2011;6:e18892. https://doi.org/10.1371/journal.pone.0018892
17. Fissore RA, Kurokawa M, Knott J, Zhang M, Smyth J. Mechanisms underlying oocyte activation and postovulatory ageing. Reproduction. 2002;124:745-54. https://doi.org/10.1530/rep.0.1240745
18. Niu YJ, Zhou W, Nie ZW, Zhou D, Xu YN, Ock SA, et al. Ubiquinol-10 delays postovulatory oocyte aging by improving mitochondrial renewal in pigs. Aging (Albany NY). 2020;12:1256-71. https://doi.org/10.18632/aging.102681
19. Tian XC, Lonergan P, Jeong BS, Evans ACO, Yang X. Association of MPF, MAPK, and nuclear progression dynamics during activation of young and aged bovine oocytes. Mol Reprod

Dev. 2002;62:132-8. https://doi.org/10.1002/mrd.10072
20. Lord T, Aitken RJ. Oxidative stress and ageing of the post-ovulatory oocyte. Reproduction. 2013;146:R217-27. https://doi.org/10.1530/REP-13-0111
21. Perez GI, Jurisicova A, Matikainen T, Moriyama T, Kim MR, Takai Y, et al. A central role for ceramide in the age-related acceleration of apoptosis in the female germline. FASEB J. 2005;19:860-2. https://doi.org/10.1096/fj.04-2903fje
22. Liang XW, Ge ZJ, Guo L, Luo SM, Han ZM, Schatten H, et al. Effect of postovulatory oocyte aging on DNA methylation imprinting acquisition in offspring oocytes. Fertil Steril. 2011;96:1479-84. https://doi.org/10.1016/j.fertnstert.2011.09.022
23. Ge ZJ, Schatten H, Zhang CL, Sun QY. Oocyte ageing and epigenetics. Reproduction. 2015;149:R103-14. https://doi.org/10.1530/REP-14-0242
24. Oktay K, Turan V, Titus S, Stobezki R, Liu L. BRCA mutations, DNA repair deficiency, and ovarian aging. Biol Reprod. 2015;93:67. https://doi.org/10.1095/biolreprod.115.132290
25. Bohrer RC, Coutinho ARS, Duggavathi R, Bordignon V. The incidence of DNA double-strand breaks is higher in late-cleaving and less developmentally competent porcine embryos. Biol Reprod. 2015;93:59. https://doi.org/10.1095/biolreprod.115.130542
26. Falck J, Mailand N, Syljuåsen RG, Bartek J, Lukas J. The ATM-Chk2-Cdc25A checkpoint pathway guards against radioresistant DNA synthesis. Nature. 2001;410:842-7. https://doi.org/10.1038/35071124
27. Panier S, Boulton SJ. Double-strand break repair: 53BP1 comes into focus. Nat Rev Mol Cell Biol. 2014;15:7-18. https://doi.org/10.1038/nrm3719
28. Burma S, Chen BP, Murphy M, Kurimasa A, Chen DJ. ATM phosphorylates histone H2AX in response to DNA double-strand breaks. J Biol Chem. 2001;276:42462-7. https://doi.org/10.1074/jbc.C100466200
29. Stiff T, Walker SA, Cerosaletti K, Goodarzi AA, Petermann E, Concannon P, et al. ATR-dependent phosphorylation and activation of ATM in response to UV treatment or replication fork stalling. EMBO J. 2006;25:5775-82. https://doi.org/10.1038/sj.emboj.7601446
30. Paull TT, Rogakou EP, Yamazaki V, Kirchgessner CU, Gellert M, Bonner WM. A critical role for histone H2AX in recruitment of repair factors to nuclear foci after DNA damage. Curr Biol. 2000;10:886-95. https://doi.org/10.1016/S0960-9822(00)00610-2
31. Bohrer RC, Duggavathi R, Bordignon V. Inhibition of histone deacetylases enhances DNA damage repair in SCNT embryos. Cell Cycle. 2014;13:2138-48. https://doi.org/10.4161/cc.29215
32. Zhang D, Zhang X, Zeng M, Yuan J, Liu M, Yin Y, et al. Increased DNA damage and repair deficiency in granulosa cells are associated with ovarian aging in rhesus monkey. J Assist Reprod Genet. 2015;32:1069-78. https://doi.org/10.1007/s10815-015-0483-5
33. Titus S, Li F, Stobezki R, Akula K, Unsal E, Jeong K, et al. Impairment of BRCA1-related DNA double-strand break repair leads to ovarian aging in mice and humans. Sci Transl Med. 2013;5:172ra21. https://doi.org/10.1126/scitranslmed.3004925
34. Zhang M, ShiYang X, Zhang Y, Miao Y, Chen Y, Cui Z, et al. Coenzyme Q10 ameliorates the quality of postovulatory aged oocytes by suppressing DNA damage and apoptosis. Free Radic Biol Med. 2019;143:84-94. https://doi.org/10.1016/j.freeradbiomed.2019.08.002
35. Park YG, Lee SE, Yoon JW, Kim EY, Park SP. Allicin protects porcine oocytes against damage during aging in vitro. Mol Reprod Dev. 2019;86:1116-25. https://doi.org/10.1002/mrd.23227
36. Lin T, Lee JE, Kang JW, Oqani RK, Cho ES, Kim SB, et al. Melatonin supplementation during prolonged in vitro maturation improves the quality and development of poor-quality porcine oocytes via anti-oxidative and anti-apoptotic effects. Mol Reprod Dev. 2018;85:665-

https://doi.org/10.5187/jast.2021.e90

81. https://doi.org/10.1002/mrd.23052
37. Livak KJ, Schmittgen TD. Analysis of relative gene expression data using real-time quantitative PCR and the 2−ΔΔCT method. Methods. 2001;25:402-8. https://doi.org/10.1006/meth.2001.1262
38. Bonner WM, Redon CE, Dickey JS, Nakamura AJ, Sedelnikova OA, Solier S, et al. γ H2AX and cancer. Nat Rev Cancer. 2008;8:957-67. https://doi.org/10.1038/nrc2523
39. Kinner A, Wu W, Staudt C, Iliakis G. γ -H2AX in recognition and signaling of DNA double-strand breaks in the context of chromatin. Nucleic Acids Res. 2008;36:5678-94. https://doi.org/10.1093/nar/gkn550
40. Zhang T, Zhang GL, Ma JY, Qi ST, Wang ZB, Wang ZW, et al. Effects of DNA damage and short-term spindle disruption on oocyte meiotic maturation. Histochem Cell Biol. 2014;142:185-94. https://doi.org/10.1007/s00418-014-1182-5
41. Yamamori T, Meike S, Nagane M, Yasui H, Inanami O. ER stress suppresses DNA double-strand break repair and sensitizes tumor cells to ionizing radiation by stimulating proteasomal degradation of Rad51. FEBS Lett. 2013;587:3348-53. https://doi.org/10.1016/j.febslet.2013.08.030
42. Govindaraj V, Keralapura Basavaraju R, Rao AJ. Changes in the expression of DNA double strand break repair genes in primordial follicles from immature and aged rats. Reprod Biomed Online. 2015;30:303-10. https://doi.org/10.1016/j.rbmo.2014.11.010
43. Bartek J, Lukas J. Chk1 and Chk2 kinases in checkpoint control and cancer. Cancer Cell. 2003;3:421-9. https://doi.org/10.1016/S1535-6108(03)00110-7
44. Reinhardt HC, Yaffe MB. Phospho-Ser/Thr-binding domains: navigating the cell cycle and DNA damage response. Nat Rev Mol Cell Biol. 2013;14:563-80. https://doi.org/10.1038/nrm3640
45. Wang ZW, Ma XS, Ma JY, Luo YB, Lin F, Wang ZB, et al. Laser microbeam-induced DNA damage inhibits cell division in fertilized eggs and early embryos. Cell Cycle. 2013;12:3336-44. https://doi.org/10.4161/cc.26327
46. Titus S, Stobezki R, Oktay K. Impaired DNA repair as a mechanism for oocyte aging: is it epigenetically determined? Semin Reprod Med. 2015;33:384-8. https://doi.org/10.1055/s-0035-1567824
47. Martin C, Zhang Y. The diverse functions of histone lysine methylation. Nat Rev Mol Cell Biol. 2005;6:838-49. https://doi.org/10.1038/nrm1761
48. Ooga M, Inoue A, Kageyama S, Akiyama T, Nagata M, Aoki F. Changes in H3K79 methylation during preimplantation development in mice. Biol Reprod. 2008;78:413-24. https://doi.org/10.1095/biolreprod.107.063453
49. Huyen Y, Zgheib O, DiTullio RA Jr., Gorgoulis VG, Zacharatos P, Petty TJ, et al. Methylated lysine 79 of histone H3 targets 53BP1 to DNA double-strand breaks. Nature. 2004;432:406-11. https://doi.org/10.1038/nature03114
50. Lin T, Lee JE, Oqani RK, Kim SY, Cho ES, Jeong YD, et al. Delayed blastocyst formation or an extra day culture increases apoptosis in pig blastocysts. Anim Reprod Sci. 2017;185:128-39. https://doi.org/10.1016/j.anireprosci.2017.08.012